

# Introducing Modelling, Analysis and Control of Three-Phase Electrical Systems Using Geometric Algebra

Manel Velasco, Isiah Zaplana, Arnau Dòria-Cerezo, Josué Duarte and Pau Martí

**Abstract**—State-of-the-art techniques for modeling, analysis and control of three-phase electrical systems belong to the real-valued multi-input/multi-output (MIMO) domain, or to the complex-valued nonlinear single-input/single-output (SISO) domain. In order to complement both domains while simplifying complexity and offering new analysis and design perspectives, this paper introduces the application of geometric algebra (GA) principles to the modeling, analysis and control of three-phase electrical systems. The key contribution for the modeling part is the identification of the transformation that allows transferring real-valued linear MIMO systems into GA-valued linear SISO representations (with independence of having a balanced or unbalanced system). Closed-loop stability analysis in the new space is addressed by using intrinsic properties of GA. In addition, a recipe for designing stabilizing and decoupling GA-valued controllers is provided. Numerical examples illustrate key developments and experiments corroborate the main findings.

**Index Terms**—Three-phase electrical systems, geometric algebra, modelling, balanced, unbalanced

## I. INTRODUCTION

THE modeling, analysis and control of three-phase electrical systems exhibits different complexity depending on the adopted representation, as sketched in Fig. 1 where a closed-loop scheme may take different forms according to the underlying space. A three-phase dynamic system can be modeled as a  $3 \times 3$  real-valued MIMO system, with a matrix of real-valued transfer functions (transfer matrix) relating each input to each output. In many applications, when either the  $\alpha\beta$  stationary frame or the  $dq$  synchronously rotating frame is adopted, the three-phase quantities can be represented by two-phase quantities and the real-valued MIMO transfer matrix is reduced by one dimension, leading to  $2 \times 2$  real MIMO systems, as illustrated in Sub-fig. 1a.

Moreover, the two-phase quantities can be organized in a complex space vector of two components, the real and imaginary parts. Then, in the complex domain, three-phase dynamic systems can be modeled using complex-valued SISO notation [1], which implies an additional reduction of the system order and moves the analysis to simpler spaces. This

allows conceptualizing alternative controllers obeying principles different than those based on real-valued models, while using extensions of control theoretical results to the complex domain, for both the analysis [2]–[6] and design phase [7]–[9].

In the complex domain, as illustrated in Sub-fig. 1b, three-phase dynamic systems modeled as SISO systems are characterized by one or two complex transfer functions (i.e., with complex coefficients) depending on whether the system is balanced or unbalanced, respectively [10], [11]. In particular, the model for unbalanced systems requires the complex conjugate of the input, which makes the SISO system nonlinear and poses difficulties in its analysis and design phases. This problem has been treated for example by neglecting the contribution of the complex conjugate input [12], or by directly applying MIMO techniques or cascaded combinations of SISO systems, in different frames ( $dq$  or  $\alpha\beta$ ) and using a variety of scalar or vector notation, e.g. [11], [13]–[17].

To overcome the previous limitations while still targeting reduced order modeling spaces, and with the objective of exploring the announced benefits of geometric algebra (GA) [18], [19], this paper introduces the use of GA principles to the modeling, analysis and control of three-phase electrical systems. It is worth noting that the application of GA to the electrical engineering field is not new. However it has been mainly bounded to the modeling of apparent power [20]–[23], power flow analysis [24], [25], and the analysis of second order systems expressed in terms of generalized coordinates [26], which differs from the current paper domain which is closed-loop control of three-phase electrical systems.

The main contribution of the paper is to show that three-phase electrical systems can be modeled in the GA domain with a linear SISO model, for both balanced and unbalanced scenarios, as shown in Sub-fig. 1c. Both the linearity and the SISO structure of the GA representation (Sub-fig. 1c) suggests an easier analysis and design phase compared to cases given by the real (Sub-fig. 1a) and complex (Sub-fig. 1b) spaces. For the modeling part, the paper presents the transformation that allows transferring  $\alpha\beta$  (or  $dq$ ) real-valued linear MIMO systems to GA-valued linear SISO systems. In the GA domain, the controller and plant that form the closed-loop system (Sub-fig. 1c) are characterized by transfer functions expressed in the GA space. Therefore, linear SISO analysis and design approaches must be reexamined. To this end, the stability of a GA closed-loop system is shown to be assessed using the same tools that apply to linear SISO real-valued systems. And regarding GA controller design, guidelines are provided

M. Velasco, J. Duarte and P. Martí are with the Automatic Control Department, Universitat Politècnica de Catalunya, Barcelona, Spain, email: {manel.velasco, josue.duarte, pau.marti}@upc.edu

I. Zaplana is with the Automatic Control Department and Inst. of Industrial and Control Engineering, Universitat Politècnica de Catalunya, Barcelona, Spain, email: isiah.zaplana@upc.edu

A. Dòria-Cerezo is with the Dept. of Electrical Engineering and Inst. of Industrial and Control Engineering, Universitat Politècnica de Catalunya, Barcelona, Spain, email: arnau.doria@upc.edu

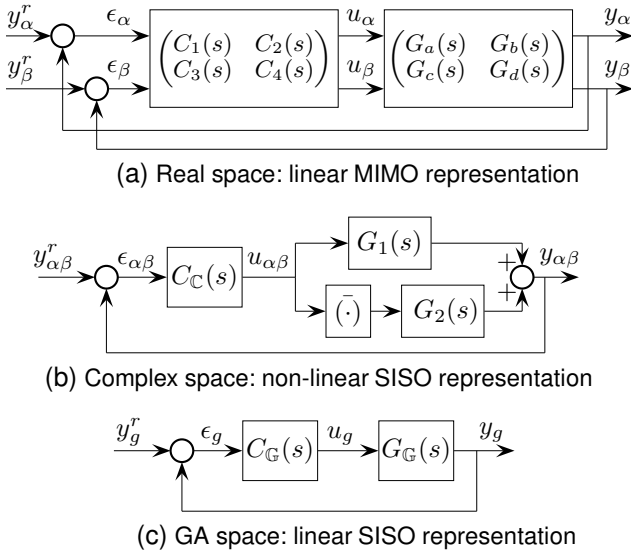


Fig. 1. Control of three-phase electrical systems in different spaces

for obtaining stabilizing controllers as well as controllers that decouple the equivalent real-valued linear closed-loop MIMO schemes. The latter is of great interest when dealing with unbalanced three-phase electrical systems.

The paper is structured as follows. Section II reviews real and complex representations of three-phase electrical systems. Section III presents the new GA modeling approach. Section IV discusses closed-loop stability and sections V and VI covers controller design. Section VII presents laboratory experiments and Section VIII concludes the paper.

**Notation.**  $\mathbb{C}^n$  and  $\mathbb{R}^n$  denote the complex and real  $n$ -dimensional space;  $\bar{x}$  denotes the conjugate of a complex vector  $x \in \mathbb{C}^n$ ;  $j \in \mathbb{C}$  is the imaginary number such that  $j^2 = -1$ ;  $\mathbb{F}$  denotes the real-valued transfer functions space and  $G(s) \in \mathbb{F}$  denotes a real-valued transfer function. For notation convenience, the space of real-valued transfer functions will also be denoted by the geometric algebra description given by  $\mathcal{F}_{0,0}$ , which is explained in detail in Appendix B. Then,  $G_{\mathbb{R}}(s) = G(s) \in \mathcal{F}_{0,0}$  denotes a real-valued transfer function, i.e.,  $\mathbb{F}$  and  $\mathcal{F}_{0,0}$  are interchangeable. Similarly, the space of complex-valued transfer functions is denoted by  $\mathcal{F}_{0,1}$  and  $G_{\mathbb{C}}(s) = G_a(s) + jG_b(s) \in \mathcal{F}_{0,1}$  denotes a complex-valued transfer function, with  $G_a(s), G_b(s) \in \mathcal{F}_{0,0}$ . Finally, the space of GA-valued transfer functions is denoted by  $\mathcal{F}_{2,0}$  and  $G_{\mathbb{G}}(s) = G_a(s)e_0 + G_b(s)e_1 + G_c(s)e_2 + G_d(s)e_{12} \in \mathcal{F}_{2,0}$  denotes a GA-valued transfer function, with  $G_a(s), G_b(s), G_c(s), G_d(s) \in \mathcal{F}_{0,0}$ .  $\bar{G}_{\mathbb{G}}(s) = G_a(s)e_0 - G_b(s)e_1 - G_c(s)e_2 - G_d(s)e_{12}$  denotes the GA conjugate of  $G_{\mathbb{G}}(s) \in \mathcal{F}_{2,0}$ . The exact meaning of the subscripts values  $p, q$  accompanying each space  $\mathcal{F}_{p,q}$  of particular transfer functions will be explained later. The term  $\underline{x}$  denotes the dual of the GA element  $x \in \mathcal{F}_{p,q}$ . Transfer function matrices whose entries are real, complex or GA-valued transfer functions belong to the  $\mathcal{F}_{p,q}^{n \times m}$  space, with appropriate values for subscripts  $p, q$ .

## II. REAL AND COMPLEX REPRESENTATION APPROACHES

Before introducing the GA modelling approach, state-of-the-art main approaches to the modelling of three phase

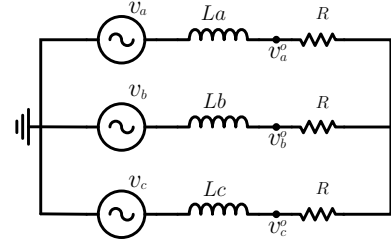


Fig. 2. Scheme for a three phase system.

electrical systems is reviewed, covering real and complex valued representations.

**Example 1** (Illustrative three-phase system). Figure 2 shows a three phase system that will be used throughout the paper to illustrate all the concepts and contributions. It is composed by three ideal voltage sources that feed a load,  $R$ , over a transmission line characterized by inductances  $L_a$ ,  $L_b$  and  $L_c$ . Depending on the values of the inductances, the system is balanced (when  $L_a = L_b = L_c = L$ ) or unbalanced (for example when  $L_a = L_c = L$  and  $L_b = L_u$ ). Whenever numerical values are provided, they correspond to the configuration given by  $L = 3 \cdot 10^{-3}H$ ,  $L_u = 3 \cdot 10^{-2}H$ ,  $R = 22\Omega$ , where voltage sinusoidal signals are characterized by an amplitude of  $V = 155$  V and a frequency of  $\omega = 2\pi 60$  rad/s.

### A. Real Representation

For the analysis and design of three-phase dynamical systems, three-phase quantities can be modeled as equivalent two-phase quantities (if zero-sequence components are disregarded) in either the  $\alpha\beta$  or  $dq$  frame. In this paper the  $\alpha\beta$  frame is adopted, but all the contributions can also be extended to the  $dq$  frame.

In the  $\alpha\beta$  frame, three-phase dynamical systems can be represented by

$$\begin{pmatrix} y_\alpha(s) \\ y_\beta(s) \end{pmatrix} = \underbrace{\begin{pmatrix} G_a(s) & G_b(s) \\ G_c(s) & G_d(s) \end{pmatrix}}_{M_{\mathbb{R}}(s)} \begin{pmatrix} u_\alpha(s) \\ u_\beta(s) \end{pmatrix} \quad (1)$$

where the system matrix  $M_{\mathbb{R}}(s)$  elements are real-valued transfer functions denoted by  $G_a(s), G_b(s), G_c(s), G_d(s) \in \mathcal{F}_{0,0}$ , and  $u = \begin{pmatrix} u_\alpha(s) & u_\beta(s) \end{pmatrix}^T \in \mathcal{F}_{0,0}^{2 \times 1}$  and  $y = \begin{pmatrix} y_\alpha(s) & y_\beta(s) \end{pmatrix}^T \in \mathcal{F}_{0,0}^{2 \times 1}$  are the input and output vectors, respectively. Recall that  $\mathcal{F}_{0,0}$  denotes the space of transfer functions with real-coefficients. The representation given by (1) will be referred to as real MIMO model and corresponds to the plant in the closed-loop scheme of Sub-fig. 1a.

**Remark 1.** For three-phase balanced systems, the real MIMO dynamics (1) have a specific structure with  $G_d(s) = G_a(s)$  and  $G_b(s) = G_c(s) = 0$ .

Remark 1 implies that the  $\alpha\beta$  channels are decoupled, thus indicating that a MIMO diagonal controller (the real-valued controller matrix in the closed-loop scheme of Sub-fig. 1a will have  $C_2(s) = C_3(s) = 0$ ) should be able to meet any feasible control performance requirement. For the unbalanced case,

the controller design problem becomes more complex because system matrix  $M_{\mathbb{R}}(s)$  in (1) is fully populated, implying that a MIMO diagonal controller may not be enough.

**Example 2** (Real MIMO: Example 1 revisited). *Applying standard modeling techniques, the real MIMO model (1) of the system of Fig. 2 for the balanced case is characterized by the system matrix*

$$M_{\mathbb{R}}(s) = \begin{pmatrix} \frac{R}{(Ls+R)} & 0 \\ 0 & \frac{R}{(Ls+R)} \end{pmatrix} \quad (2)$$

(complying with remark 1), and for the unbalanced case by

$$M_{\mathbb{R}}(s) = \begin{pmatrix} \frac{3R(2R+Ls+L_us)}{2(R+Ls)(3R+Ls+2L_us)} & \frac{-\sqrt{3}Rs(L-L_u)}{2(R+Ls)(3R+Ls+2L_us)} \\ \frac{-\sqrt{3}Rs(L-L_u)}{2(R+Ls)(3R+Ls+2L_us)} & \frac{R(6R+5Ls+L_us)}{2(R+Ls)(3R+Ls+2L_us)} \end{pmatrix} \quad (3)$$

### B. Complex Representation

The use of complex-valued dynamical models to represent three-phase electrical systems has been widely used. The linear transformation  $T_{\mathbb{C}} : \mathcal{F}_{0,0}^{2 \times 1} \rightarrow \mathcal{F}_{0,1}^{2 \times 1}$  defined by

$$\begin{pmatrix} x_{\alpha\beta}(s) \\ \bar{x}_{\alpha\beta}(s) \end{pmatrix} = T_{\mathbb{C}} \begin{pmatrix} x_{\alpha}(s) \\ x_{\beta}(s) \end{pmatrix} \quad (4)$$

with

$$T_{\mathbb{C}} = \begin{pmatrix} 1 & j \\ 1 & -j \end{pmatrix} \quad (5)$$

where  $x_{\alpha}(s), x_{\beta}(s) \in \mathcal{F}_{0,0}$  are real-valued transfer functions and  $x_{\alpha\beta}(s) = x_{\alpha}(s) + jx_{\beta}(s) \in \mathcal{F}_{0,1}$  is a complex valued transfer functions, allows transferring real-valued systems such as (1) to the complex domain [27].

The application of the transformation (4) allows transferring the real MIMO model (1) to

$$\begin{pmatrix} y_{\alpha\beta}(s) \\ \bar{y}_{\alpha\beta}(s) \end{pmatrix} = \underbrace{\begin{pmatrix} G_1(s) & G_2(s) \\ \bar{G}_2(s) & \bar{G}_1(s) \end{pmatrix}}_{M_{\mathbb{C}}(s)} \begin{pmatrix} u_{\alpha\beta}(s) \\ \bar{u}_{\alpha\beta}(s) \end{pmatrix} \quad (6)$$

where the elements of the system matrix  $M_{\mathbb{C}}(s)$  are complex-valued transfer functions denoted by  $G_1(s), G_2(s) \in \mathcal{F}_{0,1}$  and given by

$$\begin{aligned} G_1(s) &= \frac{G_a(s) + G_d(s)}{2} + j \frac{-G_b(s) + G_c(s)}{2} \\ G_2(s) &= \frac{G_a(s) - G_d(s)}{2} + j \frac{G_b(s) + G_c(s)}{2} \end{aligned} \quad (7)$$

with  $u_{\alpha\beta}(s), y_{\alpha\beta}(s) \in \mathcal{F}_{0,1}$ . Henceforth, this representation will be referred to as complex MIMO model.

**Remark 2.** *The complex MIMO model (6)-(7) exhibits a symmetry in the sense that the dynamics of the second output correspond to the dynamics of the first one in conjugate form.*

Due to the symmetry highlighted in remark 2, the analysis and design of the complex MIMO model (6)-(7) simplifies to consider only the complex-valued SISO system given by

$$y_{\alpha\beta}(s) = G_1(s)u_{\alpha\beta}(s) + G_2(s)\bar{u}_{\alpha\beta}(s) \quad (8)$$

which corresponds to the plant in the closed-loop scheme of Sub-fig. 1b, and therefore the order of the system is reduced by

half. However, dealing with (8) is, in general, a difficult task, thus challenging the design of the complex valued controller,  $C_{\mathbb{C}}(s)$  in Sub-fig. 1b. The difficulty relies on the fact that  $G_2(s)$  is multiplied by the conjugate of the input variable,  $\bar{u}_{\alpha\beta}(s)$ , introducing a non-linearity. However, this difficulty does not always hold, as explained in next remark.

**Remark 3.** *For balanced systems, in the complex MIMO dynamics (6)-(7), it holds that  $G_2(s) = 0$ . Hence, the transfer matrix is diagonal (with  $G_1$  and  $\bar{G}_1$  as diagonal elements), thus decoupling the input/output map. Hence, the complex nonlinear SISO system (8) simplifies to the linear one*

$$y_{\alpha\beta}(s) = G_1(s)u_{\alpha\beta}(s) \quad (9)$$

where  $G_1(s) = G_a(s)$  in (1).

The simplification given in remark 3 allows using existing linear SISO techniques extended to complex-valued models.

**Example 3** (Complex MIMO and SISO: Example 1 revisited). *Under the transformation (4), the real MIMO models given in (2) and (3) transform to (6)-(7) characterized by*

$$M_{\mathbb{C}}(s) = \begin{pmatrix} \frac{R+j0}{(Ls+R)} & 0+j0 \\ 0-j0 & \frac{R-j0}{(Ls+R)} \end{pmatrix} \quad (10)$$

(which complies with remark 3) for the balanced case, and for the unbalanced case by

$$M_{\mathbb{C}}(s) = \begin{pmatrix} \frac{2R(3R+2Ls+L_us)+j0}{2(R+Ls)(3R+Ls+2L_us)} & \frac{Rs(L-L_u)-j\sqrt{3}Rs(L-L_u)}{2(R+Ls)(3R+Ls+2L_us)} \\ \frac{Rs(L-L_u)+j\sqrt{3}Rs(L-L_u)}{2(R+Ls)(3R+Ls+2L_us)} & \frac{2R(3R+2Ls+L_us)-j0}{2(R+Ls)(3R+Ls+2L_us)} \end{pmatrix} \quad (11)$$

Due to the simplification obtained by the symmetry (remark 2), the control problem for the balanced case only considers the linear SISO system

$$y_{\alpha\beta}(s) = \frac{R+j0}{(Ls+R)}u_{\alpha\beta}(s) \quad (12)$$

and for the unbalanced case the nonlinear SISO system

$$\begin{aligned} y_{\alpha\beta}(s) &= \frac{2R(3R+2Ls+L_us)+j0}{2(R+Ls)(3R+Ls+2L_us)}u_{\alpha\beta}(s) \\ &+ \frac{Rs(L-L_u)-j\sqrt{3}Rs(L-L_u)}{2(R+Ls)(3R+Ls+2L_us)}\bar{u}_{\alpha\beta}(s) \end{aligned} \quad (13)$$

### III. GEOMETRIC ALGEBRA REPRESENTATION

The representation of the real MIMO system (1) in the geometric algebra domain is also obtained by applying a particular transformation to the real representation. However, before presenting the transformation, and intuitive approach to the geometric algebra representation is given.

#### A. Intuitive approach to the geometric algebra representation

By applying linear matrix algebra (see appendix A for the full development), the transfer matrix  $M_{\mathbb{R}}(s)$  of the real MIMO system (1) can be decomposed as

$$\begin{aligned} M_{\mathbb{R}}(s) &= \frac{G_a(s)+G_d(s)}{2} \begin{pmatrix} 1 & 0 \\ 0 & 1 \end{pmatrix} + \frac{G_a(s)-G_d(s)}{2} \begin{pmatrix} 1 & 0 \\ 0 & -1 \end{pmatrix} \\ &+ \frac{G_b(s)+G_c(s)}{2} \begin{pmatrix} 0 & 1 \\ 1 & 0 \end{pmatrix} + \frac{G_b(s)-G_c(s)}{2} \begin{pmatrix} 0 & 1 \\ -1 & 0 \end{pmatrix} \end{aligned} \quad (14)$$

The decomposition given in (14) can be rewritten, and with an abuse of notation, renamed, as

$$G_{\mathbb{G}}(s) = \frac{G_a(s) + G_d(s)}{2}e_0 + \frac{G_a(s) - G_d(s)}{2}e_1 + \frac{G_b(s) + G_c(s)}{2}e_2 + \frac{G_b(s) - G_c(s)}{2}e_{12} \quad (15)$$

where

$$\{e_0, e_1, e_2, e_{12}\} = \left\{ \begin{pmatrix} 1 & 0 \\ 0 & 1 \end{pmatrix}, \begin{pmatrix} 1 & 0 \\ 0 & -1 \end{pmatrix}, \begin{pmatrix} 0 & 1 \\ 1 & 0 \end{pmatrix}, \begin{pmatrix} 0 & 1 \\ -1 & 0 \end{pmatrix} \right\} \quad (16)$$

The definition of  $G_{\mathbb{G}}(s)$  in (15) can be explained as defining a transfer function whose structure is a linear combination of the four basis elements (16), whose coefficients are the particular transfer functions that appear in (15).

It is also interesting to highlight that the elements of the basis (16) exhibit the following properties

$$\begin{aligned} e_1^2 &= \begin{pmatrix} 1 & 0 \\ 0 & -1 \end{pmatrix} \begin{pmatrix} 1 & 0 \\ 0 & -1 \end{pmatrix} = \begin{pmatrix} 1 & 0 \\ 0 & 1 \end{pmatrix} \\ e_2^2 &= \begin{pmatrix} 0 & 1 \\ 1 & 0 \end{pmatrix} \begin{pmatrix} 0 & 1 \\ 1 & 0 \end{pmatrix} = \begin{pmatrix} 1 & 0 \\ 0 & 1 \end{pmatrix} \\ e_1 e_2 &= \begin{pmatrix} 1 & 0 \\ 0 & -1 \end{pmatrix} \begin{pmatrix} 0 & 1 \\ 1 & 0 \end{pmatrix} = \begin{pmatrix} 0 & 1 \\ -1 & 0 \end{pmatrix} \\ e_{12}^2 &= \begin{pmatrix} 0 & 1 \\ -1 & 0 \end{pmatrix} \begin{pmatrix} 0 & 1 \\ -1 & 0 \end{pmatrix} = \begin{pmatrix} -1 & 0 \\ 0 & -1 \end{pmatrix} \end{aligned} \quad (17)$$

That is, if we denoted the identity matrix by  $e_0$ ,  $e_1$  and  $e_2$  squares to the identity matrix ( $e_0$ ), and  $e_1 e_2$  is a new element, denoted by  $e_{12}$  and that behaves like the imaginary complex unit  $j$ , i.e., it squares to minus the identity ( $-e_0$ ).

More specifically,  $G_{\mathbb{G}}(s)$  in (15) can be identified as an element that belongs to a 4-dimensional geometric algebra which is spanned by the four basis elements  $\{e_0, e_1, e_2, e_{12}\}$  in (16). And each element in this geometric algebra is called a multivector which is a linear combination of the basis elements whose coefficients belong to the space of real-valued transfer functions. The four basis elements are called scalar,  $e_0$  (often omitted because it is the identity), vectors  $e_1$  and  $e_2$ , and bivector or pseudoscalar  $e_{12}$ . The particular form of this geometric algebra is condensed in the notation  $\mathcal{F}_{2,0}$  (which is further explained in appendix B).

Next section derives a representation of the real MIMO system (1) in the GA domain with decoupled dynamics.

### B. A $\mathcal{F}_{2,0}$ representation

The specific representation of the real MIMO system (1) in the geometric algebra  $\mathcal{F}_{2,0}$ , partially introduced in subsection III-A, is not unique (analogous to the complex case) and it will depend on the transformation being applied. This section presents a transformation that decouples the input/outputs maps and leaves them in the linear domain, both for balanced and unbalanced systems. Moreover, it achieves a symmetry that simplifies the whole analysis to a GA linear SISO system.

The original real MIMO model (1) is transferred to the new  $\mathcal{F}_{2,0}$  geometric algebra space by applying the following linear transformation  $T_{\mathbb{G}} : \mathcal{F}_{0,0}^2 \rightarrow (\mathcal{F}_{2,0})^2$  defined by

$$\begin{pmatrix} x_g(s) \\ \underline{x}_g(s) \end{pmatrix} = T_{\mathbb{G}} \begin{pmatrix} x_{\alpha}(s) \\ x_{\beta}(s) \end{pmatrix} \quad (18)$$

with

$$T_{\mathbb{G}} = \frac{1}{2} \begin{pmatrix} e_0 + e_1 & e_2 - e_{12} \\ e_2 + e_{12} & e_0 - e_1 \end{pmatrix} \quad (19)$$

where  $\{e_0, e_1, e_2, e_{12}\}$  is given in (16),  $x_{\alpha}(s), x_{\beta}(s) \in \mathcal{F}_{0,0}$  are real-valued transfer functions,  $x_g(s) = \frac{1}{2}(x_{\alpha}(s)e_0 + x_{\alpha}(s)e_1 + x_{\beta}(s)e_2 - x_{\beta}(s)e_{12}) \in \mathcal{F}_{2,0}$ , and  $\underline{x}_g(s) \in \mathcal{F}_{2,0}$  stands for the dual of  $x_g(s)$  and it is given by  $\underline{x}_g(s) = x_g(s)e_{12}$  [29].

Hence, the application of (18) to the real MIMO system (1) leads to

$$\begin{pmatrix} y_g(s) \\ \underline{y}_g(s) \end{pmatrix} = \underbrace{\begin{pmatrix} G_{\mathbb{G}}(s) & 0 \\ 0 & G_{\mathbb{G}}(s) \end{pmatrix}}_{M_{\mathbb{G}}(s)} \begin{pmatrix} u_g(s) \\ \underline{u}_g(s) \end{pmatrix} \quad (20)$$

where  $u_g(s), y_g(s) \in \mathcal{F}_{2,0}$ , and the system matrix  $M_{\mathbb{G}}(s)$  elements are geometric-valued transfer functions:  $G_{\mathbb{G}}(s) \in \mathcal{F}_{2,0}$  was already given in (15), and the zeros of the contra-diagonal stand for  $0 = 0e_0 + 0e_1 + 0e_2 + 0e_{12} \in \mathcal{F}_{2,0}$ , i.e., multivectors of  $\mathcal{F}_{2,0}$ . Henceforth, this representation will be referred to as geometric MIMO model.

**Remark 4.** It can be observed that the transformation (18) is involutive, i.e.,  $T_{\mathbb{G}} = T_{\mathbb{G}}^{-1}$ , property that will be used in Section VI.

**Remark 5.** As it can be observed in the geometric algebra representation (20), the transformation (18) decouples the input/output map because the system matrix is diagonal. Moreover, since both diagonal elements are equal, the analysis and design of the geometric algebra system (20) simplifies to consider only the linear geometric-valued SISO system

$$y_g(s) = G_{\mathbb{G}}(s)u_g(s) \quad (21)$$

Differently from what happens in the complex case, remark 5 indicates that no matter whether the real MIMO system (1) is balanced or unbalanced, the geometric MIMO system (20) permits facing the controller analysis and design focusing only on the linear geometric SISO case (21), which corresponds to the plant of the closed-loop scheme of Subfig. 1c.

**Example 4** (Geometric MIMO and SISO: Example 1 revisited). Under the transformation (18), the real MIMO model given in (2) and (3) transform to (20) characterized by

$$\begin{aligned} M_{\mathbb{G}}(s) &= \begin{pmatrix} \frac{m_b(s)}{Ls+R} & 0 \\ 0 & \frac{m_b(s)}{Ls+R} \end{pmatrix} \\ m_b(s) &= Re_0 + 0e_1 + 0e_2 + 0e_{12} \end{aligned} \quad (22)$$

for the balanced case, and for the unbalanced case by

$$M_{\mathbb{G}}(s) = \begin{pmatrix} \frac{m_u(s)}{2(R+Ls)(3R+Ls+2L_us)} & 0 \\ 0 & \frac{m_u(s)}{2(R+Ls)(3R+Ls+2L_us)} \end{pmatrix}$$

$$m_u(s) = 2R(3R + 2Ls + L_us)e_0 - R(L - L_u)se_1 - \sqrt{3}R(L - L_u)se_2 + 0e_{12} \quad (23)$$

Since both representations (22) and (23) comply with remark 5, the control problem for the balanced and unbalanced case only has to consider the linear SISO systems

$$y_g(s) = \frac{m_b(s)}{Ls + R} u_g(s) \quad (24)$$

and

$$y_g(s) = \frac{m_u(s)}{2(R + Ls)(3R + Ls + 2L_us)} u_g(s) \quad (25)$$

It is of interest to outline that the elements of the transfer matrix of the geometric MIMO system (20) (and consequently the geometric SISO case (21)) are multivectors in terms of the four basis elements (16), whose coefficients are real-valued transfer functions, as illustrated in (22) and (23).

#### IV. GA STABILITY ANALYSIS

Since the analysis and controller design problem of the geometric MIMO model (20) is reduced to a geometric SISO model (21) (recall remark 5) characterized by  $G_{\mathbb{G}}(s)$  (15), the closed-loop scheme of interest simplifies to the one shown in Sub-fig. 1c, where a controller  $C_{\mathbb{G}}(s) \in \mathcal{F}_{2,0}$  must be designed for the plant  $G_{\mathbb{G}}(s) \in \mathcal{F}_{2,0}$  in such a way that closed-loop stability is ensured.

The closed-loop transfer function for the scheme shown in Sub-fig. 1c is given by

$$G_{cl}(s) = G_{\mathbb{G}}(s)C_{\mathbb{G}}(s)(e_0 + G_{\mathbb{G}}(s)C_{\mathbb{G}}(s))^{-1} \quad (26)$$

Assume that the plant and controller,  $G_{\mathbb{G}}$  and  $C_{\mathbb{G}}$  respectively, are expressed in a numerator/denominator structure as follows

$$G_{\mathbb{G}}(s) = \frac{n_p(s)}{d_p(s)} \quad \text{and} \quad C_{\mathbb{G}}(s) = \frac{n_c(s)}{d_c(s)} \quad (27)$$

where  $n_p(s), d_p(s), n_c(s), d_c(s) \in \mathcal{F}_{2,0}$ , and specifically, where the denominators  $d_p(s)$  and  $d_c(s)$  have only scalar part. Note that it is always possible to manipulate the quotients given in (27) in such a way that they can be expressed in terms of denominators given only by a real-valued transfer functions (that is, having  $d_p(s), d_c(s) \in \mathbb{F} \equiv \mathcal{F}_{0,0}$ ).

**Proposition 1.** *The closed-loop scheme shown in Sub-fig. 1c, whose transfer function is given in (26), and where the controller and plant are denoted by  $C_{\mathbb{G}}(s), G_{\mathbb{G}}(s) \in \mathcal{F}_{2,0}$ , and decomposed as in (27), is asymptotically stable if the zeros of a real-valued polynomial  $d_{cl}(s) \in \mathcal{F}_{0,0}$  given by*

$$d_{cl}(s) = \overline{d_{pc}(s)}d_{pc}(s) \quad (28)$$

with

$$d_{pc}(s) = d_p(s)d_c(s) + n_p(s)n_c(s) \in \mathcal{F}_{2,0} \quad (29)$$

have negative real part.

*Proof.* By using (27) and a few algebraic operations, the closed-loop transfer function (26) can be further written as

$$G_{cl}(s) = \frac{n_p(s)}{d_p(s)} \frac{n_c(s)}{d_c(s)} \left( e_0 + \frac{n_p(s)}{d_p(s)} \frac{n_c(s)}{d_c(s)} \right)^{-1}$$

$$= \frac{n_p(s)}{d_p(s)} \frac{n_c(s)}{d_c(s)} \left( \frac{d_p(s)d_c(s) + n_p(s)n_c(s)}{d_p(s)d_c(s)} \right)^{-1}$$

$$= \frac{n_p(s)}{d_p(s)} \frac{n_c(s)}{d_c(s)} \left( \frac{d_{pc}(s)}{d_p(s)d_c(s)} \right)^{-1} = n_p(s)n_c(s)(d_{pc}(s))^{-1}$$

$$= n_p(s)n_c(s) \frac{\overline{d_{pc}(s)}}{d_{pc}(s)d_{pc}(s)} = \frac{n_p(s)n_c(s)\overline{d_{pc}(s)}}{d_{pc}(s)d_{pc}(s)} \quad (30)$$

From (30), it can be observed that the denominator of the closed-loop transfer function  $G_{cl}(s)$ , announced in (28), by using Property 1 stated in appendix B, is a real-valued transfer function,  $d_{pc}(s)d_{pc}(s) \in \mathbb{R}$ . Hence, its zeros will determine closed-loop system stability.  $\square$

In consequence, and focusing on Sub-fig. 1c, when designing a geometric controller  $C_{\mathbb{G}}(s) \in \mathcal{F}_{2,0}$  for the geometric plant,  $G_{\mathbb{G}}(s) \in \mathcal{F}_{2,0}$ , the closed-loop stability is analyzed using the same tools used in real-valued systems. That is, studying the poles of the closed-loop system which are the roots of the real polynomial denominator.

**Example 5** (Stability analysis for Example 4). *Assume the following geometric proportional controller*

$$C_{\mathbb{G}} = k(e_0 + e_1), \quad k \in \mathbb{R} \quad (31)$$

for the unbalanced geometric representation of the plant (25) in closed-loop form as in Sub-fig. 1c. The closed-loop transfer function (26) is given by

$$G_{cl}(s) = \left( \frac{3kR(2R + Ls + L_us)}{d_{cl}(s)} \right) e_0$$

$$+ \left( \frac{3kR(2R + Ls + L_us)}{d_{cl}(s)} \right) e_1$$

$$+ \left( -\frac{\sqrt{3}kRs(L - L_u)}{d_{cl}(s)} \right) e_2$$

$$+ \left( \frac{\sqrt{3}kRs(L - L_u)}{d_{cl}(s)} \right) e_{12} \quad (32)$$

where

$$d_{cl}(s) = (2L^2 + 4L_uL)s^2$$

$$+ (6kLR + 8LR + 6kL_uR + 4L_uR)s$$

$$+ 12kR^2 + 6R^2 \quad (33)$$

It is interesting to note that the denominator (33) is a real-valued polynomial, as discussed in Proposition 1. Within the discussion, and for illustrative purposes, it is of interest to show that  $d_{pc}(s)$  (29) is given by

$$d_{pc}(s) = ((2L^2 + 4L_uL)s^2$$

$$+ (3kLR + 8LR + 3kL_uR + 4L_uR)s$$

$$+ 6kR^2 + 6R^2) e_0 + (3kR(2R + Ls + L_us)) e_1$$

$$+ (-\sqrt{3}kRs(L - L_u)) e_2 + (\sqrt{3}kRs(L - L_u)) e_{12} \quad (34)$$

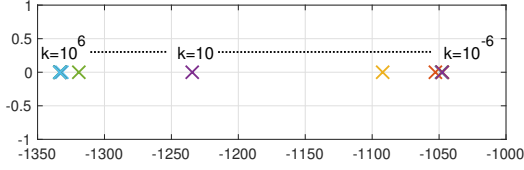


Fig. 3. Location of the slowest closed-loop system pole as a function of  $k$

The zeros of (33) with the numerical values for the components given in Example 1 and  $k = 10$  are  $s_1 = -1.22 \cdot 10^5$  and  $s_2 = -0.01 \cdot 10^5$ . Hence, according to Proposition 1, the closed-loop systems is stable. In fact, Figure 3 shows the location for the slowest pole of the closed-loop system (32) as a function of a wider range of values for the controller gain:  $k$  in (31), with  $k = 10^{-6} \cdot 10^i$ ,  $i = 0, 1, 2, 3, 4$ . For any value, stability is guaranteed (the real part of the pole is always negative), and for small values of  $k$ , the pole value collapses around  $-1.04 \cdot 10^3$  and for high values, it collapses around  $-1.33 \cdot 10^3$ .

**Example 6** (More on stability analysis). By doing the same analysis of Example 5 (with the unbalanced geometric representation of the plant (25)) but with the following slightly different proportional controller than (31)

$$C_{\mathbb{G}} = k(e_1 + e_2), \quad k \in \mathbb{R} \quad (35)$$

it can be concluded that the closed-loop system is unstable because the denominator of the closed-loop transfer function has a zero with positive real part,  $s = 0.14 \cdot 10^5$ .

## V. AN INTERPRETATION OF GA CONTROLLER DESIGN

This section illustrates possible benefits of applying a geometric algebra-based approach to the problem of designing controllers for three-phase electrical systems. It must be stressed that any design performed in the GA domain has an equivalent in the real domain (by simply applying the inverse of the transformation presented in (4)). Note that this equivalence also applies between the real and the complex domain. The novelty of using GA relies on the intrinsic different perspectives and paradigms that the GA domain offer, in addition to the inherent benefits of working with a plant characterized for being SISO and linear (20).

The controller design phase for real MIMO systems (illustrated in Sub-fig. 1a) involves three main steps: input/output pairing, decoupling, and controller design. The objective of pairing and decoupling is making the overall closed-loop transfer function of the controlled real MIMO system diagonal, which relates to a structural objective. And the controller design objective is to meet the control requirements, which relates to a performance objective.

In the geometric algebra domain, the analysis and controller design phase must be performed on a linear SISO plant (20), whose generic expression can be given by

$$G_{\mathbb{G}}(s) = g_0(s)e_0 + g_1(s)e_1 + g_2(s)e_2 + g_3(s)e_{12} \quad (36)$$

In closed-loop form, as illustrated in Sub-fig. 1c, the controller can also be generically expressed as

$$C_{\mathbb{G}}(s) = c_0(s)e_0 + c_1(s)e_1 + c_2(s)e_2 + c_3(s)e_{12} \quad (37)$$

Hence, the existing pairing and decoupling algorithms for real MIMO systems does not apply in the GA domain. However, noting that there is a correspondence between the real and GA spaces given by the presented transformation (18), it seems reasonable to assert that the pairing and decoupling in the GA space depends on the coefficients of the controller,  $c_0(s)$ ,  $c_1(s)$ ,  $c_2(s)$  and  $c_3(s)$ .

Following this line, and going to the simplest scenario, assume for the geometric controller (37) the proportional form

$$C_{\mathbb{G}}(s) = ke_0, \quad k \in \mathbb{R} \quad (38)$$

Hence, the closed-loop form (26) where the controller is given by (38) and the plant is given by (36) is

$$G_{cl}(s) = \frac{n_{cl}(s)}{d_{cl}(s)} \quad (39)$$

where

$$\begin{aligned} n_{cl}(s) &= k^2 (g_0^2(s) - g_1^2(s) - g_2^2(s) + g_3^2(s)) e_0 \\ &\quad + k (g_0(s)e_0 + g_1(s)e_1 + g_2(s)e_2 + g_3(s)e_{12}) \\ d_{cl}(s) &= k^2 (g_0^2(s) - g_1^2(s) - g_2^2(s) + g_3^2(s)) + 2kg_0(s) + 1 \end{aligned} \quad (40)$$

Before analyzing structural or performance properties of the geometric closed-loop form (39)-(40), some known facts of the real domain are reminded. First, for real linear SISO stable plants, the higher the value for the proportional gain of a proportional controller, the lower the steady state error. And second, when the gain tends towards infinity, the real SISO closed-loop transfer function is the identity, and the reference signal is copied to the output (i.e., ideal performance). Hence, it is of interest to study the behavior of the geometric closed-loop system (39)-(40) when  $k \rightarrow \infty$ , which is given by

$$\lim_{k \rightarrow \infty} G_{cl}(s) = 1e_0 + 0e_1 + 0e_2 + 0e_{12} \quad (41)$$

Surprisingly, in (41) a double effect can be identified. First, the fact that all basis coefficients are zero except for  $e_0$  implies that the equivalent real MIMO closed-loop system (obtained through transformation (18)) is diagonal, that is, decoupled. Therefore, the achievement of a diagonal form suggests that increasing the value of the gain  $k$  of the proportional GA controller (38) has a decoupling effect in the real domain, which covers the structural objective. And second, being the coefficient of  $e_0$  equal to one in (41) implies that the equivalent real MIMO closed-loop system is exactly the identity matrix, which means that the ideal performance notion is kept under the geometric algebra domain if it is stable, which covers the steady-state error objective.

It is worth noting that having a single geometric proportional controller for the other basis elements different than  $e_0$  (used in (38)) have the same structural effects. That is, the following geometric controllers

$$C_{\mathbb{G}}(s) = ke_i, \quad i \in \{1, 2, 12\}, \quad k \in \mathbb{R} \quad (42)$$

have the same decoupling effect. However, the performance objective is not always kept. Only  $C_{\mathbb{G}}(s) = ke_0$  or  $C_{\mathbb{G}}(s) = ke_{12}$  result in a stable closed-loop system (by applying Proposition 1) and therefore they can provide ideal performance if  $k \rightarrow \infty$ . However,  $C_{\mathbb{G}}(s) = ke_1$  or  $C_{\mathbb{G}}(s) = ke_2$  leads to

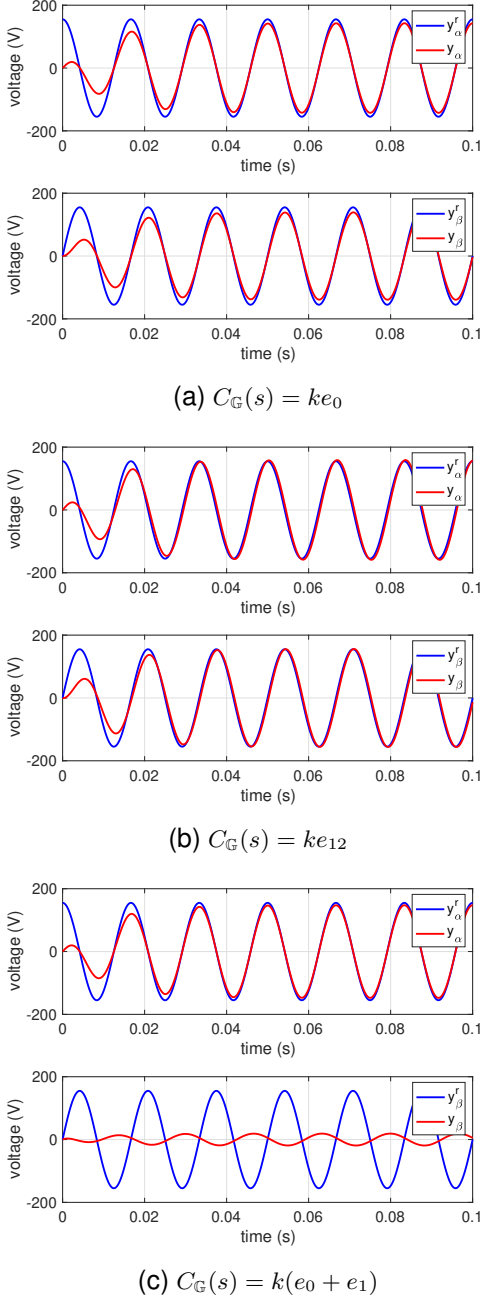


Fig. 4. Simulations of the stable controllers of Example 6 with  $k = 10$ .

unstable dynamics and ideal performance is not possible. Just for illustrative purposes, the real-valued controllers that are obtained from the proportional geometric controllers (38) and (42) applying the inverse of the transformation (18) (and that populate  $C_1(s)$ ,  $C_2(s)$ ,  $C_3(s)$ , and  $C_4(s)$  of the controller matrix in the real MIMO closed-loop of Sub-fig. (1a)) are

$$\begin{matrix} ke_0 & ke_1 & ke_2 & ke_{12} \\ \updownarrow & \updownarrow & \updownarrow & \updownarrow \\ \begin{pmatrix} k & 0 \\ 0 & k \end{pmatrix} & \begin{pmatrix} k & 0 \\ 0 & -k \end{pmatrix} & \begin{pmatrix} 0 & k \\ k & 0 \end{pmatrix} & \begin{pmatrix} 0 & k \\ -k & 0 \end{pmatrix} \end{matrix} \quad (43)$$

It is interesting to also note that the controller (31) used in Example 5,  $C_G(s) = k(e_0 + e_1)$ , which was stable is not a

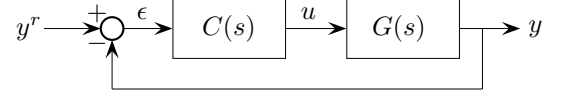


Fig. 5. Closed-loop scheme

diagonalizing (decoupling) controller (the application of (41) gives a multivector where all basis coefficients are different than zero) and therefore the closed-loop output will not meet a given reference set-point but will settle to a particular value. Again, just for illustrative purposes, the real MIMO equivalent of this proportional geometric controller is

$$k(e_0 + e_1) \leftrightarrow \begin{pmatrix} 2k & 0 \\ 0 & 0 \end{pmatrix} \quad (44)$$

**Example 7** (Closed-loop simulations). *For the stable controllers of Example 6, with  $k = 10$ , Figure 4 shows their performance when the closed-loop output (red lines) track two sinusoidal reference signals (blue lines) for each  $\alpha\beta$  channel, which can be condensed in polar form by  $r(t) = e^{j\omega t}$ ,  $\omega = 2\pi 60$  rad/s. Sub-fig. 4a and 4b shows the performance of the proportional controllers given in (38) and in (42) (for  $i = 12$ ), which apart from being stable, also tend to decouple the closed-loop dynamics. Both sub-figures show similar tracking performance. The first one exhibits an amplitude error while the second one exhibits a phase error. Both errors decrease for higher values of  $k$ . Complementary, Sub-fig. 4c shows the performance of the proportional controllers given in (35), which is stable but not tending to decouple the closed-loop dynamics. As it can be observed, tracking is achieved in the  $\alpha$  channel but not the  $\beta$  one.*

## VI. STABILIZING AND DECOUPLING GA CONTROLLERS

### A. Stabilizing GA-valued controllers

This section presents a new tool for the analysis and controller design by extending the  $Q$  parameterization (or Youla parameterization [34]) of all stabilizing controllers to the GA domain. In the real domain, the Youla parametrization states that for the closed-loop scheme of Figure 5 where the plant  $G(s)$  is a stable transfer function matrix, the family of all stabilizing negative feedback controllers is given by

$$C(s) = (I - Q(s)G(s))^{-1} Q(s) \quad (45)$$

where the parameter  $Q(s)$  is a stable and proper transfer function matrix.

**Proposition 2.** *Assume that for the real-valued closed-loop scheme shown in Fig. 5 the family of all real-valued stabilizing negative feedback controllers  $C(s)$  is given by (45), where the plant  $G(s)$  is stable, and the parameter  $Q(s)$  is stable and proper. Then, for the GA-valued closed-loop scheme shown in Sub-fig. 1c, the family of all geometric-valued stabilizing negative feedback controllers  $C_G(s)$  is given by*

$$C_G(s) = (I - Q_G(s)G_G(s))^{-1} Q_G(s) \quad (46)$$

where  $C_G(s) = T_G C(s) T_G$ ,  $G_G(s) = T_G G(s) T_G$ , and  $Q_G(s) = T_G Q(s) T_G$ , with the transformation  $T_G$  in (18).



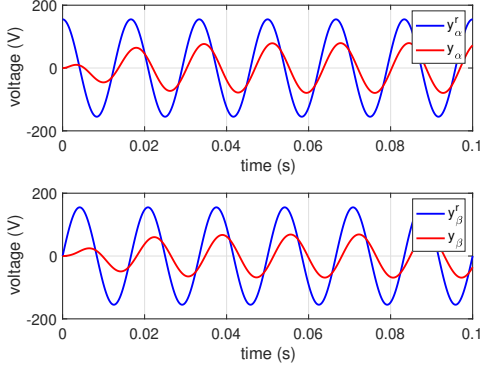


Fig. 6. Stabilizing controller

*Proof.* By applying the transformation (18) to (45), the following expression is obtained

$$T_{\mathbb{G}}^{-1}C(s)T_{\mathbb{G}} = T_{\mathbb{G}}^{-1}(I - Q(s)G(s))^{-1}Q(s)T_{\mathbb{G}} \quad (47)$$

By using the involutivity property highlighted in Remark 4, expression (47) can be written as

$$T_{\mathbb{G}}C(s)T_{\mathbb{G}} = T_{\mathbb{G}}(I - Q(s)T_{\mathbb{G}}T_{\mathbb{G}}G(s))^{-1}T_{\mathbb{G}}T_{\mathbb{G}}Q(s)T_{\mathbb{G}} \quad (48)$$

and rearranged as

$$\underbrace{T_{\mathbb{G}}C(s)T_{\mathbb{G}}}_{C_{\mathbb{G}}(s)} = (I - \underbrace{T_{\mathbb{G}}Q(s)T_{\mathbb{G}}}_{Q_{\mathbb{G}}}\underbrace{T_{\mathbb{G}}G(s)T_{\mathbb{G}}}_{G_{\mathbb{G}}})^{-1}\underbrace{T_{\mathbb{G}}Q(s)T_{\mathbb{G}}}_{Q_{\mathbb{G}}} \quad (49)$$

which leads to (46).  $\square$

Hence, in the GA domain, Proposition 2 indicates that for a given plant, the family of stabilizing controllers can be computed using the same procedure that applies to the real domain.

**Example 8** (Stabilizing a geometric controller for Example 4). *Considering the unbalanced geometric representation of the plant (25) in closed-loop form as in Sub-fig. 1c, and considering*

$$Q_{\mathbb{G}}(s) = \frac{a}{s+b}e_0 \quad (50)$$

with  $a = b = 500$ , as the stable and proper transfer function acting as a free parameter for the family of all geometric-valued stabilizing negative feedback controllers given in (46), leads to

$$\begin{aligned} C_{\mathbb{G}}(s) = & \frac{500s^2 + 4.44 \cdot 10^6 s + 4.889 \cdot 10^9}{s^3 + 9381s^2 + 1.212 \cdot 10^7 s} e_0 \\ & + \frac{3.929 \cdot 10^8}{s^3 + 9381s^2 + 1.212 \cdot 10^7 s} e_1 \\ & + \frac{6.804 \cdot 10^8}{s^3 + 9381s^2 + 1.212 \cdot 10^7 s} e_2 \end{aligned} \quad (51)$$

The closed-loop dynamics are shown in Fig. 6, which clearly show coupling between the  $\alpha\beta$  channels. In fact, it is easy to double check that the equivalent real MIMO closed-loop transfer matrix is not diagonal (decoupled).

## B. Decoupling Parametrization

From the geometric-based parametrization (46) for all stabilizing controllers, this section presents design conditions on the  $Q_{\mathbb{G}}(s)$  parameter such that the corresponding stabilizing geometric controller achieves a decoupled real MIMO closed-loop system. By substituting in the closed-loop expression (26) the controller by (46), the geometric closed-loop description using the parametrization of stabilizing controllers is given by

$$S_{\mathbb{G}}(s) = G_{\mathbb{G}}(s)Q_{\mathbb{G}}(s) \quad (52)$$

In GA, any decoupled plant can be described as

$$S_{\mathbb{G}}(s) = S_0(s)e_0 \quad (53)$$

which corresponds to

$$S(s) = \begin{pmatrix} S_0(s) & 0 \\ 0 & S_0(s) \end{pmatrix} \quad (54)$$

in the real-domain. Hence, a decoupled plant (53) in the GA domain demands having the coefficients of  $e_1$ ,  $e_2$  and  $e_{12}$  equal to zero. Considering the generic form for the plant  $G_{\mathbb{G}}(s)$  (36) and a generic form for the free parameter  $Q_{\mathbb{G}}(s)$  given by

$$Q_{\mathbb{G}}(s) = q_0(s)e_0 + q_1(s)e_1 + q_2(s)e_2 + q_3(s)e_{12} \quad (55)$$

then the closed-loop description (52) can be written as

$$\begin{aligned} S_{\mathbb{G}}(s) = & G_{\mathbb{G}}(s)Q_{\mathbb{G}}(s) \\ = & (g_0(s)q_0(s) + g_1(s)q_1(s) + g_2(s)q_2(s) - g_3(s)q_3(s))e_0 \\ & + (g_0(s)q_1(s) + g_1(s)q_0(s) - g_2(s)q_3(s) + g_3(s)q_2(s))e_1 \\ & + (g_0(s)q_2(s) + g_2(s)q_0(s) + g_1(s)q_3(s) - g_3(s)q_1(s))e_2 \\ & + (g_0(s)q_3(s) + g_1(s)q_2(s) - g_2(s)q_1(s) + g_3(s)q_0(s))e_{12} \end{aligned} \quad (56)$$

Forcing the coefficients of  $e_1$ ,  $e_2$  and  $e_{12}$  to be zero in (56) leads to a system of 3 equations with 4 unknowns which have infinite solutions, that will depend on  $q_0(s)$ ,  $q_1(s)$ ,  $q_2(s)$  or  $q_3(s)$ . For example, taking  $q_0(s)$  as a free parameter, then the rest of parameters that decouple the closed-loop form (56) leading to (53) are  $q_1(s) = -\frac{g_1(s)q_0(s)}{g_0(s)}$ ,  $q_2(s) = -\frac{g_2(s)q_0(s)}{g_0(s)}$  and  $q_3(s) = -\frac{g_3(s)q_0(s)}{g_0(s)}$ .

**Example 9** (Decoupling a geometric controller for Example 4). *Considering the unbalanced geometric representation of the plant (25) in closed-loop form as in Sub-fig. 1c, in order to compute the free parameter  $Q_{\mathbb{G}}(s)$  for the family of all geometric-valued stabilizing negative feedback controllers given in (46) that decouple the real-MIMO dynamics, the parameter  $q_0(s)$  is chosen to be*

$$q_0(s) = 1 \quad (57)$$

which transforms (55) to

$$Q_{\mathbb{G}}(s) = 1e_0 + \frac{(L - L_u)s}{(4L + 2L_u)s + 6R}e_1 + \frac{\sqrt{3}(L - L_u)s}{(4L + 2L_u)s + 6R}e_2 \quad (58)$$

which is stable and proper. By considering (58) rather than (50) used in the previous example as the free parameter, the parametrization (46) leads to

$$C_{\mathbb{G}}(s) = \frac{3s + 5500}{3s}e_0 + \frac{-3}{8}e_1 + \frac{-3\sqrt{3}}{8}e_2 \quad (59)$$



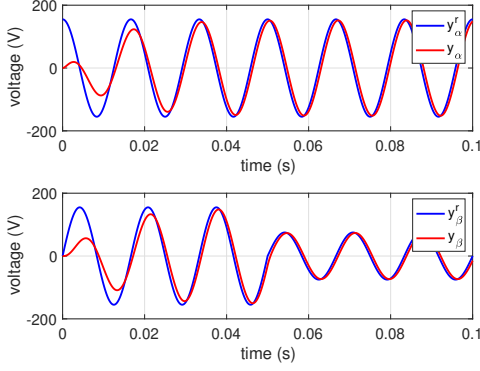


Fig. 7. Decoupling controller.

and the closed-loop dynamics are shown in Fig. 7, which clearly show the desired decoupling between the  $\alpha\beta$  channels. To further illustrate the decoupling, a voltage reference set-point change has been introduced at time  $t = 0.04$  s only for the  $\beta$  channel that becomes transparent for the  $\alpha$  channel. In fact, it is easy to double check that the equivalent real MIMO closed-loop transfer matrix is diagonal. Note that in Fig. 7 perfect tracking is not achieved because the design procedure just presented only imposes decoupling, that is, a real-MIMO transfer function matrix with diagonal shape (54). To have perfect tracking,  $S_0(s)$  should be forced to be the identity.

**Example 10** (Proportional Controller as a Decoupling Geometric controller for Example 4). Section V presented the proportional controller (38) as a decoupling controller leading to the identity  $1e_0$  according to (41) when  $k \rightarrow \infty$ . This example assess whether this proportional controller is compliant with the family of stabilizing and decoupling controllers. In order to compute the free parameter  $Q_G(s)$  for the stabilizing negative feedback controller given in (46) that decouples the real-MIMO dynamics while leading to the identity  $1e_0$ , by using (52), it must follow that

$$G_G(s)Q_G(s) = 1e_0 \rightarrow Q_G(s) = G_G(s)^{-1} \quad (60)$$

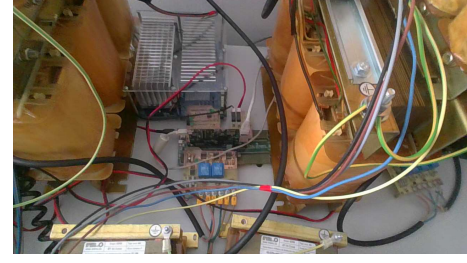
Then, by substituting (60) in the controller given in (46) it is obtained

$$\begin{aligned} C_G(s) &= (I - G_G(s)Q_G(s))^{-1} Q_G(s) \\ &= (I - I)^{-1} G_G(s)^{-1} \\ &= \infty e_0 \end{aligned} \quad (61)$$

which indeed is the proportional controller given in (38) for  $k = \infty$

## VII. EXPERIMENTS

The three phase scheme shown in Fig. 2 has been reproduced in the laboratory to test the proposed controller (see Figure 8). The voltage source is implemented using a MTL-CBI0060F12IXHF GUASCH three-phase IGBT full-bridge power inverter with a rated power of 3.3 kVA at 110 V<sub>rms</sub> and 10 A<sub>rms</sub> (central card in Sub-fig. 8a). The inductances and load were given in Example 1. The unbalanced load is composed by three heaters (one per line), and one line has an



(a) Inverter



(b) Unbalanced load

Fig. 8. Laboratory set-up.

additional inductance for creating the imbalance (Sub-fig. 8b). The input of the inverter is supplied by a Cinergia B2C+DC power source. The decoupling controller (59) is implemented at the inverter on the F28M36 digital signal processor (DSPs) from Texas Instruments and executed every  $T_s = 100 \mu s$ .

Fig. 9 shows the main results for the unbalanced case ( $L_a = L_c$  and  $L_b = L_u$ ), for both the open-loop (Sub-fig. 9a) and closed-loop (Sub-fig. 9b) scenarios. For each scenario, the top graph shows the three-phase currents,  $i_a$ ,  $i_b$  and  $i_c$ , and the two graphs below show the tracking performance (voltage reference and output voltage for each  $\alpha\beta$  channel).

For the open-loop scenario, Sub-fig. 9a, the currents are clearly unbalanced, and voltage tracking performance is lost. The application of the decoupling controller (59) in the closed-loop scenario, Sub-fig. 9b, achieves, apart from stable dynamics, balanced currents and decoupled voltage tracking dynamics.

## VIII. CONCLUSIONS

Motivated by limitations that traditional modelling approaches have for unbalanced systems, this paper has introduced the use of geometric algebra for the dynamic modelling, analysis and controller design of three-phase dynamical systems. The modelling approach, based on a new transformation, allows representing either balanced and unbalanced three phase electrical systems with a single GA-valued linear SISO model. Moreover, it has been shown that the stability analysis in the new geometric domain simplifies to analyzing the roots of a real-valued polynomial, as it is also done in the case of standard real-valued linear SISO models. Regarding the controller design phase, the Youla parametrization has been extended to the geometric algebra domain for the design of stable and decoupling controllers. Future work will further investigate on additional geometric algebra based modelling, analysis and controller design tools.

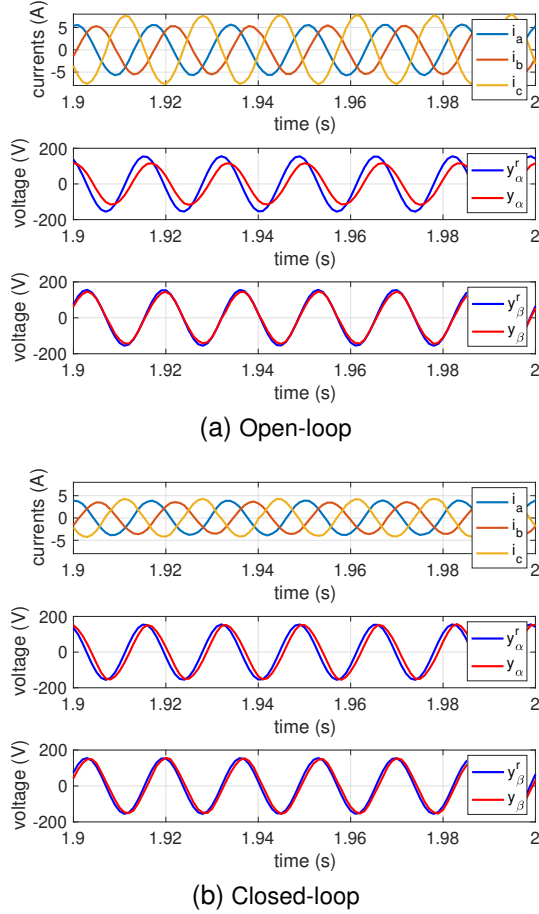


Fig. 9. Geometric controller experiment.

#### APPENDIX A REAL MIMO MATRIX DECOMPOSITION

The Toeplitz decomposition is applied to the transfer function matrix  $M_{\mathbb{R}}(s)$  of the real MIMO system (1), that states that every square matrix is the sum in a unique way of a symmetric and a skew-symmetric matrix [28], leading to

$$M_{\mathbb{R}}(s) = \underbrace{\frac{M_{\mathbb{R}}(s) + M_{\mathbb{R}}(s)^T}{2}}_{M_s(s)} + \underbrace{\frac{M_{\mathbb{R}}(s) - M_{\mathbb{R}}(s)^T}{2}}_{M_a(s)} \quad (62)$$

where  $M_s(s)$  and  $M_a(s)$  denote the symmetric and the skew-symmetric matrices, respectively. By adding and subtracting the trace of  $M_{\mathbb{R}}(s)$  (divided by 2) in (62), the following expression for  $M_{\mathbb{R}}(s)$  is obtained

$$M_{\mathbb{R}}(s) = \frac{T_r(M_{\mathbb{R}}(s))}{2}I + \underbrace{M_s(s) - \frac{T_r(M_{\mathbb{R}}(s))}{2}I}_{M_t(s)} + M_a(s) \quad (63)$$

which, by adding and subtracting a diagonal matrix whose elements are the diagonal elements of  $M_t(s)$ , can be further written as

$$M_{\mathbb{R}}(s) = \frac{T_r(M_{\mathbb{R}}(s))}{2}I + D_g(M_t(s)) + \underbrace{M_t(s) - D_g(M_t(s))}_{M_v(s)} + M_a(s) \quad (64)$$

The decomposition of  $M_{\mathbb{R}}(s)$  given in (64), considering the original definition given in (1), permits to define

$$\begin{aligned} \frac{T_r(M_{\mathbb{R}}(s))}{2}I &= \frac{1}{2} \begin{pmatrix} G_a(s) + G_d(s) & 0 \\ 0 & G_a(s) + G_d(s) \end{pmatrix} \\ D_g(M_t(s)) &= \frac{1}{2} \begin{pmatrix} G_a(s) - G_d(s) & 0 \\ 0 & G_d(s) - G_a(s) \end{pmatrix} \\ M_v(s) &= \frac{1}{2} \begin{pmatrix} 0 & G_b(s) + G_c(s) \\ G_b(s) + G_c(s) & 0 \end{pmatrix} \\ M_a(s) &= \frac{1}{2} \begin{pmatrix} 0 & G_b(s) - G_c(s) \\ G_c(s) - G_b(s) & 0 \end{pmatrix} \end{aligned} \quad (65)$$

which allows re-writing (64) into the expression given in (14).

#### APPENDIX B GEOMETRIC ALGEBRA BASIC CONCEPTS

In general, let  $\mathbb{R}^{p+q}$  be a real vector space, where  $p$  and  $q$  are the number of basis vectors that square to 1 and  $-1$ , respectively, i.e., the dimension of this real vector space is  $n = p + q$ . The associated geometric algebra  $\mathcal{G}_{p,q}(\mathbb{R})$  has  $2^n$  basis elements, and the objects of this algebra, called multivectors, are linear combinations of them, where the coefficients belong to  $\mathbb{R}$ . The core idea of geometric algebra is its multiplication operation, called the geometric product, which is the sum of an inner and an outer product [29]. Every geometric algebra  $\mathcal{G}_{p,q}(\mathbb{R})$  has as scalar basis element, which is denoted by  $e_0$ , and plays the role of the identity for the geometric product.

If instead of  $\mathbb{R}^{p+q}$ , an arbitrary vector space over a field is considered, the associated geometric algebra is constructed in an analogous manner.

**Example 11** (Real numbers). *The geometric algebra representation of the real numbers space,  $\mathbb{R}$ , is given by  $\mathcal{G}_{0,0}(\mathbb{R})$ , or simply  $\mathcal{G}_{0,0}$ , where the only basis element is  $e_0$ . Hence,  $a \in \mathbb{R}$  can be represented as  $ae_0 \in \mathcal{G}_{0,0}$*

**Example 12** (Complex numbers). *The geometric algebra representation of the complex numbers space,  $\mathbb{C}$ , is given by  $\mathcal{G}_{0,1}(\mathbb{R})$ , or simply  $\mathcal{G}_{0,1}$ , where the only basis element besides  $e_0$  is  $e_1 = j$  (that squares  $-1$ ). Hence,  $a + jb \in \mathbb{C}$ , with  $a, b \in \mathbb{R}$ , can be represented as  $ae_0 + be_1 \in \mathcal{F}_{0,1}$ .*

**Example 13** (Complex-valued transfer functions). *The geometric algebra representation of the complex-valued transfer functions space is given by  $\mathcal{G}_{0,1}(\mathbb{F})$ , or  $\mathcal{F}_{0,1}$  to distinguish it from the geometric algebra representation of the complex numbers. Its basis elements are  $e_0$  and  $e_1 = j$ . Hence, the complex-valued transfer function  $G_a(s) + jG_b(s)$  with  $G_a(s), G_b(s) \in \mathbb{F}$  can be represented as  $G_a(s)e_0 + G_b(s)e_1 \in \mathcal{F}_{0,1}$ .*

**Example 14** (Geometric-valued transfer functions). *The geometric algebra representation of the geometric-valued transfer functions space is given by  $\mathcal{G}_{2,0}(\mathbb{F})$ , or simply  $\mathcal{F}_{2,0}$ . Its basis elements are  $e_0, e_1, e_2$  and  $e_1e_2 = e_{12}$ , where  $e_1e_2$  denotes the geometric product between vectors  $e_1$  and  $e_2$ . Hence, a geometric-valued transfer function can be represented as  $G_a(s)e_0 + G_b(s)e_1 + G_c(s)e_2 + G_d(s)e_{12} \in \mathcal{F}_{2,0}$  with  $G_a(s), G_b(s), G_c(s), G_d(s) \in \mathbb{F}$ , i.e., real-valued transfer functions.*

It is worth noting that the decomposition given in (14) is an example of the fact that any  $2 \times 2$  matrix can be represented as a linear combination of the four basis components (16), which implies that the geometric algebra  $\mathcal{F}_{2,0}$  is isomorphic to the algebra of  $2 \times 2$  matrices over the field of real-valued transfer functions [33].

Below, the extension of a known property of GA to the particular geometric algebra  $\mathcal{F}_{2,0}$  that is used in the stability analysis is announced. It states that the product of a multivector  $m(s) \in \mathcal{F}_{2,0}$  by its geometric conjugate gives a scalar real-valued transfer function.

**Property 1.** Assume the following generic expression for a multivector  $m(s) = a(s)e_0 + b(s)e_1 + c(s)e_2 + d(s)e_{12} \in \mathcal{F}_{2,0}$ , with  $a(s), b(s), c(s), d(s) \in \mathcal{F}_{0,0}$  and  $\{e_0, e_1, e_2, e_{12}\}$  given in (16). Since its geometric conjugate is given by  $\bar{m}(s) = a(s)e_0 - b(s)e_1 - c(s)e_2 - d(s)e_{12}$  [31], it follows that

$$\bar{m}(s)m(s) = a(s)^2 - b(s)^2 - c(s)^2 + d(s)^2 \quad (66)$$

which is a real-valued transfer function in  $s$ , that is,  $\bar{m}(s)m(s) \in \mathcal{F}_{0,0}$ .

## REFERENCES

- [1] L. Harnefors, "Modeling of three-phase dynamic systems using complex transfer functions and transfer matrices," *IEEE Transactions on Industrial Electronics*, vol. 54, no. 4, pp. 2239-2248, Aug. 2007.
- [2] E. Frank, "On the zeros polynomials with complex coefficients," *Bulletin of the American Mathematical Society*, vol. 5, no. 2, pp. 144-157, 1946.
- [3] N. Bose and Y. Shi, "A simple general proof of Kharitonov's generalized stability criterion," *IEEE Transactions on Circuits and Systems*, vol. 34, no. 10, pp. 1233-1237, October 1987.
- [4] S. Gataric and N. R. Garrigan, "Modeling and design of three-phase systems using complex transfer functions", 30th Annual IEEE Power Electron. Specialists Conference, vol. 2, pp. 691-697, 1999.
- [5] A. Dòria-Cerezo and M. Bodson, "Design of controllers for electrical power systems using a complex root locus method", *IEEE Transactions on Industrial Electronics*, vol. 63, no. 6, pp. 3706-3716, Jun. 2016.
- [6] O. Troeng, B. Bernhardsson and C. Rivetta, "Complex-coefficient systems in control", Proceedings of the American Control Conference, pp. 1721-1727, 2017.
- [7] X. Guo, W. Wu and Z. Chen, "Multiple-complex coefficient-filter-based phase-locked loop and synchronization technique for three-phase grid-interfaced converters in distributed utility networks", *IEEE Transactions on Industrial Electronics*, vol. 58, no. 4, pp. 1194-1204, Apr. 2011.
- [8] H. J. Baesmat and M. Bodson, "Pole placement control for doubly-fed induction generators using compact representations in complex variables", *IEEE Transactions on Energy Conversion*, vol. 34, no. 2, pp. 750-760, Jun. 2019.
- [9] A. Dòria-Cerezo, J. M. Olm, D. Biel and E. Fossas, "Sliding Modes in a Class of Complex-Valued Nonlinear Systems", *IEEE Transactions on Automatic Control*, vol. 66, no. 7, pp. 3355-3362, 2021.
- [10] K. W. Martin, "Complex signal processing is not complex," *IEEE Transactions on Circuits and Systems I: Regular Papers*, vol. 51, no. 9, pp. 1823-1836, Sept. 2004.
- [11] L. Harnefors, X. Wang, S.-F. Chou, M. Bongiorno, M. Hinkkanen and M. Routimo, "Asymmetric Complex-Vector Models With Application to VSC-Grid Interaction," in *IEEE Journal of Emerging and Selected Topics in Power Electronics*, vol. 8, no. 2, pp. 1911-1921, June 2020.
- [12] L. Harnefors, X. Wang, A. G. Yepes and F. Blaabjerg, "Passivity-based stability assessment of grid-connected VSCs—an overview", *IEEE Journal of Emerging and Selected Topics in Power Electronics*, vol. 4, no. 1, pp. 116-125, Mar. 2016.
- [13] A. Rygg, M. Molinas, C. Zhang and X. Cai, "A modified sequence-domain impedance definition and its equivalence to the dq-domain impedance definition for the stability analysis of AC power electronic systems", *IEEE Journal of Emerging and Selected Topics in Power Electronics*, vol. 4, no. 4, pp. 1383-1396, Dec. 2016.
- [14] A. Rygg, M. Molinas, C. Zhang and X. Cai, "On the equivalence and impact on stability of impedance modeling of power electronic converters in different domains", *IEEE Journal of Emerging and Selected Topics in Power Electronics*, vol. 5, no. 4, pp. 1444-1454, Dec. 2017.
- [15] X. Wang, L. Harnefors and F. Blaabjerg, "Unified impedance model of grid-connected voltage-source converters," *IEEE Transactions on Power Electronics*, vol. 33, no. 2, pp. 1775-1787, Feb. 2018.
- [16] C. Zhang, X. Cai, A. Rygg and M. Molinas, "Sequence domain SISO equivalent models of a grid-tied voltage source converter system for small-signal stability analysis," *IEEE Transactions on Energy Conversion*, vol. 33, no. 2, pp. 741-749, June 2018.
- [17] C. Zhang, M. Molinas, A. Rygg and X. Cai, "Impedance-based analysis of interconnected power electronics systems: impedance network modeling and comparative studies of stability criteria," *IEEE Journal of Emerging and Selected Topics in Power Electronics*, vol. 8, no. 3, pp. 2520-2533, Sept. 2020.
- [18] J. M. Chappell et al., "Geometric Algebra for Electrical and Electronic Engineers," in *Proceedings of the IEEE*, vol. 102, no. 9, pp. 1340-1363, Sept. 2014.
- [19] E. Bayro-Corrochano, "A Survey on Quaternion Algebra and Geometric Algebra Applications in Engineering and Computer Science 1995–2020," in *IEEE Access*, vol. 9, pp. 104326-104355, 2021.
- [20] A. Menti, T. Zacharias and J. Miliadis-Argitis, "Geometric Algebra: A Powerful Tool for Representing Power Under Nonsinusoidal Conditions," in *IEEE Transactions on Circuits and Systems I: Regular Papers*, vol. 54, no. 3, pp. 601-609, March 2007.
- [21] M. Castilla, J. C. Bravo, M. Ordonez and J. C. Montano, "Clifford Theory: A Geometrical Interpretation of Multivectorial Apparent Power," in *IEEE Transactions on Circuits and Systems I: Regular Papers*, vol. 55, no. 10, pp. 3358-3367, Nov. 2008.
- [22] M. Castro-Núñez, R. Castro-Puche and E. Nowicki, "The use of geometric algebra in circuit analysis and its impact on the definition of power," 2010 International School on Nonsinusoidal Currents and Compensation, Lagow, Poland, pp. 89-95, 2010.
- [23] M. Castro-Nunez and R. Castro-Puche, "Advantages of Geometric Algebra Over Complex Numbers in the Analysis of Networks With Nonsinusoidal Sources and Linear Loads," in *IEEE Transactions on Circuits and Systems I: Regular Papers*, vol. 59, no. 9, pp. 2056-2064, Sept. 2012.
- [24] F.G. Montoya and A.H. Eid, "Formulating the geometric foundation of Clarke, Park, and FBD transformations by means of Clifford's geometric algebra", *Mathematical Methods in the Applied Sciences*, vol. 45, no. 8, pp. 4252- 4277, 2022.
- [25] A. H. Eid and F. G. Montoya, "A Systematic and Comprehensive Geometric Framework for Multiphase Power Systems Analysis and Computing in Time Domain," in *IEEE Access*, vol. 10, pp. 132725-132741, 2022.
- [26] S.D. Garvey, M.I. Friswell and J.E.T. Penny, "Clifford Algebraic Perspective on Second-Order Linear Systems" *Journal of Guidance, Control, and Dynamics*, vol. 24, n. 1, pp. 35-45, 2001.
- [27] J. Undrill and T. Kostyniak, "Subsynchronous oscillations part 1- Comprehensive system stability analysis," *IEEE Transactions on Power Apparatus and Systems*, vol. 95, no. 4, p. 1446-1455, 1976.
- [28] S. Andrilli and D. Hecker, *Elementary Linear Algebra*, 5th Edition, Academic Press, 2016.
- [29] D. Hestenes and G. Sobczyk, *Clifford Algebra to Geometric Calculus*, Dordrecht: Springer Netherlands, 1984.
- [30] D. S. Shirokov, "Concepts of trace, determinant and inverse of Clifford algebra elements", Proc. of the 8th Congress of the International Society for Analysis, its Applications, and Computation, pp 187-194, 2011.
- [31] E. Hitzer and S. Sangwine, "Multivector and multivector matrix inverses in real Clifford algebras", *Applied Mathematics and Computation*, vol. 311, pp. 375-389, 2017.
- [32] A. Timbus, M. Liserre, R. Teodorescu, P. Rodriguez and F. Blaabjerg, "Evaluation of Current Controllers for Distributed Power Generation Systems," *IEEE Transactions on Power Electronics*, vol. 24, no. 3, pp. 654-664, March 2009.
- [33] P. Lounesto, *Clifford Algebra and Spinors*, Cambridge Univ. Press, Cambridge, England, U.K., pp. 1 - 49, 1997.
- [34] D. Youla, H. Jabr and J. Bongiorno, "Modern Wiener-Hopf design of optimal controllers-Part II: The multivariable case," *IEEE Transactions on Automatic Control*, vol. 21, no. 3, pp. 319-338, June 1976.